ACS OMEGA

http://pubs.acs.org/journal/acsodf

Article

Rhodamine B-Conjugated Fluorescent Block Copolymer Micelles for Efficient Chlorambucil Delivery and Intracellular Imaging

Bhagyashree Kulkarni, Somayah Qutub, Niveen M. Khashab,* and Nikos Hadjichristidis*

Cite This: *ACS Omega* 2023, 8, 22698−22707

Read Online

ACCESS | Metrics & More | Article Recommendations | Supporting Information

ABSTRACT: The clinical development of the anticancer drug chlorambucil (CHL) is limited by its low solubility in water, poor bioavailability, and off-target toxicity. Besides, another constraint for monitoring intracellular drug delivery is the non-fluorescent nature of CHL. Nanocarriers based on block copolymers of poly(ethylene glycol)/poly(ethylene oxide) (PEG/PEO) and poly(ε-caprolactone) (PCL) are an elegant choice for drug delivery applications due to their high biocompatibility and inherent biodegradability properties. Here, we have designed and prepared block copolymer micelles (BCM) containing CHL (BCM-CHL) from a block copolymer having fluorescent probe rhodamine B (RhB) end-groups to achieve efficient drug delivery and intracellular imaging. For this purpose, the previously reported tetraphenylethylene (TPE)-containing poly(ethylene oxide)-*b*-poly(ε-caprolactone) [TPE-(PEO-*b*-PCL)$_2$] triblock copolymer was conjugated with RhB by a feasible and effective post-polymerization modification method. In addition, the block copolymer was obtained by a facile and efficient synthetic strategy of one-pot block copolymerization. The amphiphilicity of the resulting block copolymer TPE-(PEO-*b*-PCL-RhB)$_2$ led to the spontaneous formation of micelles (BCM) in aqueous media and successful encapsulation of the hydrophobic anticancer drug CHL (CHL-BCM). Dynamic light scattering and transmission electron microscopy analyses of BCM and CHL-BCM revealed a favorable size (10−100 nm) for passive targeting of tumor tissues *via* the enhanced permeability and retention effect. The fluorescence emission spectrum (λ_{ex} 315 nm) of BCM demonstrated Förster resonance energy transfer between TPE aggregates (donor) and RhB (acceptor). On the other hand, CHL-BCM revealed TPE monomer emission, which may be attributed to the $\pi-\pi$ stacking interaction between TPE and CHL molecules. The *in vitro* drug release profile showed that CHL-BCM exhibits drug release in a sustained manner over 48 h. A cytotoxicity study proved the biocompatibility of BCM, while CHL-BCM revealed significant toxicity to cervical (HeLa) cancer cells. The inherent fluorescence of RhB in the block copolymer offered an opportunity to directly monitor the cellular uptake of the micelles by confocal laser scanning microscopy imaging. These results demonstrate the potential of these block copolymers as drug nanocarriers and as bioimaging probes for theranostic applications.

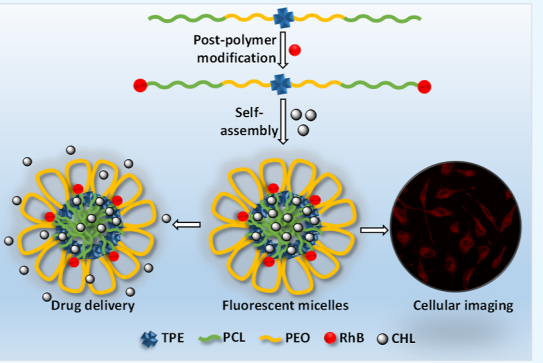

INTRODUCTION

Chemotherapy remains a prominent modality among conventional cancer therapies in current clinical practice. Chlorambucil (CHL) is one of the important chemotherapeutic drugs frequently used for treating many cancers, including chronic lymphocytic leukemia,[1] breast cancer,[2] and ovarian cancer.[3] CHL is an aromatic nitrogen mustard DNA alkylating agent and exerts its toxicity through the reaction of its two reactive chloroethyl side chains selectively with the N7 position of guanine bases inducing intra- and inter-strand crosslinking in DNA,[4] which interferes in the DNA replication and ultimately leads to cell apoptosis.[5] However, despite its DNA alkylating potency, poor solubility, short *in vivo* half-life due to rapid degradation in plasma,[6] and severe off-target toxicity[7,8] limit its clinical progress. In this regard, developing polymeric nanocarriers is one of the most promising strategies to improve aqueous solubility and half-life and increase drug accumulation at the target site, thereby reducing systemic toxicity for safe and enhanced chemotherapeutic efficacy.[9−13]

However, the inherent nonfluorescent nature of CHL hampers the monitoring of cellular uptake and intracellular drug release by fluorescence microscopy; thus, it is challenging to understand its dynamic status through *in vitro* studies. To this end, significant efforts have been made to introduce fluorescent molecules, including pyrene,[14] coumarin,[15,16] 1,8-naphthalamide,[17,18] rhodamine B,[19,20] and nile red,[21] into the polymeric drug nanocarriers to help monitor the non-fluorescent CHL drug delivery process. Thus, various fluorescent drug delivery systems have been developed for CHL delivery. However, most of these nanocarriers are based

Received: March 6, 2023
Accepted: April 25, 2023
Published: June 14, 2023

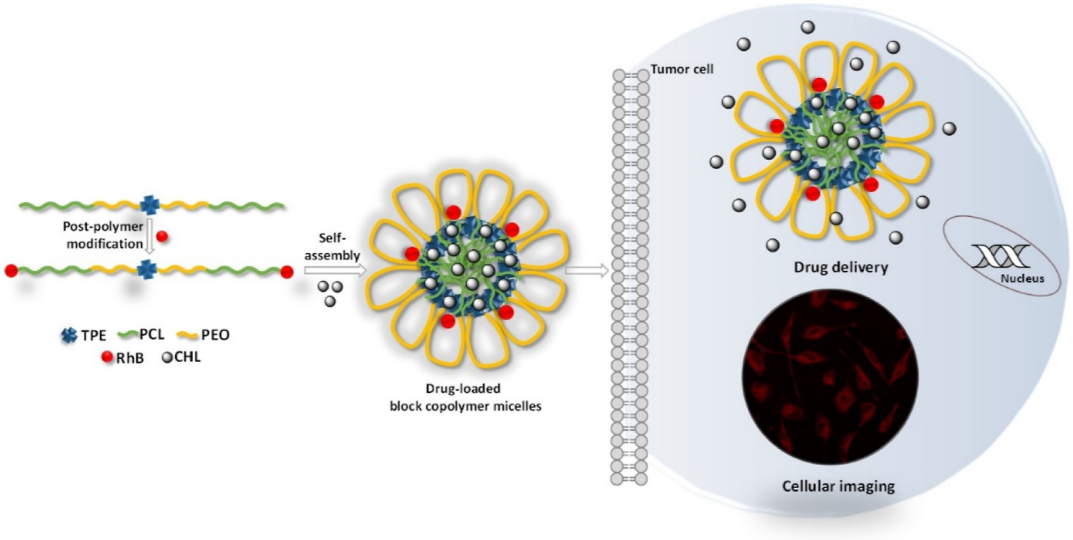

Figure 1. Schematic illustration of the RhB-conjugated BCM for CHL drug delivery and intracellular imaging.

on non-biodegradable polymeric materials, which could limit their *in vivo* studies. Although biodegradability is highly desirable for drug delivery applications, only a few studies report the use of a biodegradable polymer segment[16,20] into the fluorescent drug delivery systems for CHL. On the other hand, fluorescent polymeric drug delivery systems encounter limitations such as laborious synthetic procedures,[14,15,17,18] inefficient drug release,[14,17] and notorious aggregation-caused quenching of fluorophores in the nanoaggregates.[14,21] Therefore, we sought to develop a feasible preparation of fluorescent block copolymer micelles based on poly(ε-caprolactone) (PCL) and poly(ethylene oxide) (PEO) for CHL encapsulation along with a rhodamine B (RhB) fluorescent probe, which assists in monitoring the *in vitro* CHL delivery. Nanocarriers based on block copolymers of poly(ethylene glycol)/PEO and PCL are an elegant choice for drug delivery applications due to their high biocompatibility and inherent biodegradability properties. In addition, the block copolymer was obtained by a facile and efficient synthetic strategy of one-pot block copolymerization followed by simple post-polymerization modification. For this purpose, the triblock copolymer TPE-(PEO-*b*-PCL)$_2$ was synthesized by a facile one-pot, initiated by tetraphenylethylene (TPE) fluorophore, block copolymerization, which we previously reported.[22] The synthesized triblock copolymer was further end-functionalized with RhB *via* an easy post-polymerization modification [TPE-(PEO-*b*-PCL-RhB)$_2$]. The RhB was anchored at the chain-end of the block copolymer to take advantage of the Förster resonance energy transfer (FRET) between TPE (donor) and RhB (acceptor) as a probe for real-time monitoring of the drug delivery process at the cellular level.[23] However, interestingly, it was found that the encapsulation of CHL in the block copolymer micelles (BCM) reduced the energy transfer effect. Even so, RhB was exploited as a fluorescent probe to promote the cellular imaging of the CHL-loaded micelles thanks to its excellent optical properties.[24] The present CHL-encapsulated drug delivery system (schematically depicted in Figure 1) has the following advantages: (i) the aqueous solubility of the drug is significantly improved as the drug is accommodated in the hydrophobic core of the micelles; (ii) the drug-loaded micelles (CHL-BCM) showed sustained drug release and can achieve selective tumor targeting due to enhanced permeability and retention (EPR) effect;[25] (iii) the MTT assay confirmed the biocompatibility of the BCM, while the CHL-loaded micelles demonstrated a cytotoxic effect in the cervical (HeLa) cancer cells; (iv) RhB enabled the visualization of cellular uptake of the micelles by confocal laser scanning microscopy (CLSM) imaging, revealing effective internalization and accumulation at the cytoplasm. Thus, the present approach accomplishes simultaneous intracellular drug delivery and imaging of the nonfluorescent drug.

EXPERIMENTAL SECTION

Materials. CHL, RhB, 4-(dimethylamino) pyridine (DMAP), and 1-ethyl-3-(3-dimethylaminopropyl)-carbodiimide hydrochloride (EDC·HCL) were purchased from Sigma-Aldrich. Methanol, tetrahydrofuran (THF), diethyl ether, acetone, hexane, and ethyl acetate were purchased from VWR Chemicals. Dichloromethane (anhydrous, ≥99%) was purchased from Sigma-Aldrich. All the chemicals and solvents were used as received without any further purification—Dulbecco's modified eagle's medium (DMEM), fetal bovine serum (FBS), penicillin−streptomycin, 0.05% trypsin−EDTA, and 1× phosphate-buffered saline (PBS). Human cervical cancer cell line (HeLa) and human dermal fibroblast (HDF) were purchased from American Type Culture Collection (ATCC, Manassas, VA, USA). T75 cell culture flasks (Thermo Scientific) and 96-well plates (Corning Incorporated) were used. The cell cytotoxicity assay kit (ab112118) was purchased from Abcam.

Measurements. NMR measurements were performed at room temperature using a Bruker AVANCE III-500 MHz spectrometer instrument in $CDCl_3$ solvent. Size exclusion chromatography was performed on an Agilent liquid chromatography instrument equipped with two similar PL gel columns connected in series and two detectors, namely, a refractive index detector and a UV−Vis detector. DMF was used as a mobile phase (containing 0.005 M LiBr) at a flow rate of 1 mL min^{-1} at 45 °C, and the polymer concentration was 2 mg mL^{-1}. The instrument was calibrated with polystyrene standards. UV−Vis absorption spectra were recorded on a Thermo Evolution 600 UV−visible spectropho-

https://doi.org/10.1021/acsomega.3c01514
ACS Omega 2023, 8, 22698−22707

tometer. Fluorescence emission spectra were recorded using a Horiba Jobin Yvon Fluoromax-4 spectrofluorometer. Dynamic light scattering (DLS) measurements were carried out at 25 °C using a Malvern Zetasizer Nano ZS instrument equipped with a 30 mW He−Ne laser light source emitting vertically polarized light of 632.8 nm wavelength (scattering angle 173°). Transmission electron microscopy images were recorded on an FEI-Technai Twin instrument operated at 120 kV in the bright-field mode. The aqueous solution of the sample (1 mg mL^{-1}) was drop-cast on a carbon-coated copper grid followed by staining with uranyl acetate (2%).

Synthesis of TPE-(PEO-*b*-PCL-RhB)$_2$. In a round-bottom flask, triblock copolymer TPE-(PEO-*b*-PCL)$_2$ ($M_{n,NMR}$ = 11.8 kg mol^{-1}) (0.5 g, 42.3 μmol) was dissolved in dry CH_2Cl_2 (4.0 mL) under an argon atmosphere. Subsequently, RhB (60.8 mg, 0.12 mmol), EDC·HCl (24.3 mg, 0.12 mmol), and a catalytic amount of DMAP were added to the flask, and the reaction mixture was stirred at room temperature for 48 h. The polymer solution was precipitated (three times) into a 1:1 (v/v) mixture of diethyl ether and methanol. Further, the polymer was dialyzed (MWCO = 3500 Da) against water to remove the unreacted RhB and the product was obtained as a crimson-red powder after freeze-drying. Yield: 95%. ^{1}H NMR (500 MHz, $CDCl_3$): δ ppm 7.09−6.63 (m, aromatic proton), 6.89 (m, 4H), 6.63 (m, 4H), 4.06 (t, 2H) 3.64 (m, 4H), 2.31 (t, 2H) 1.65 (t, 4H), 1.38 (t, 2H). ($M_{n,NMR}$ = 12.1 kg mol^{-1}, $Đ_{SEC}$ = 1.18).

Triblock Copolymer Micelle (BCM) Preparation and CHL Loading (CHL-BCM). The BCM were prepared by a co-solvent evaporation method.[26] The block copolymer (1.0 mg) was dissolved in acetone (1.0 mL), and deionized water was added dropwise (1.0 mL) at room temperature under stirring. After thoroughly removing the organic solvent by rotary vacuum evaporation at room temperature, the solution was filtered through a nylon syringe filter (0.22 μm pore size) to obtain the BCM. CHL-encapsulated micelles (CHL-BCM) were prepared following a similar procedure by adding CHL to the polymer solution. The concentration of CHL was determined based on the absorbance at 258 nm measured by a UV−Visible spectrophotometer against a standard calibration curve. The drug loading content (DLC) and the drug loading efficiency (DLE) were calculated according to the following equations[27]

$$\mathrm{DLC}(\%) = \frac{\text{weight of drug encapsulated in nanoparticles}}{\text{weight of drug loaded nanoparticles}} \times 100$$

$$\mathrm{DLE}(\%) = \frac{\text{weight of drug encapsulated in nanoparticles}}{\text{weight of drug in feed}} \times 100$$

Stability of CHL-BCM. The stability of CHL-BCM was examined in PBS (pH 7.4) and PBS (pH 7.4) containing 10% FBS at a concentration of 0.1 mg mL^{-1} at 37 °C. At various time points, the particle size of micelle samples was monitored by DLS over a period of 48 h.

In Vitro Drug Release. The drug release study was performed at 37 °C in PBS of pH 7.4, 6.8, and 5.5. To improve the limited water solubility of CHL in PBS, a solution containing PBS and acetonitrile (95:5 v/v) was used to determine drug release. As already reported, the solubility of the released hydrophobic drug in PBS can be improved by the use of co-solvents such as ethanol, methanol, acetonitrile, and DMSO.[14,28,29] CHL-loaded micelle solution (1.0 mL) was sealed in a semipermeable membrane (Spectra/Por MWCO 3500) and dialyzed against the buffer solution. Subsequently, at specific time intervals, 2.0 mL of the release medium was withdrawn to measure the absorbance at 258 nm by a UV−Visible spectrophotometer. The concentration of the CHL released from the micelles was calculated from the calibration curve (Supporting Information).

Cytotoxicity Studies. HeLa cells and HDF were maintained in DMEM media supplemented with 10% (v/v) FBS and 1% (v/v) penicillin−streptomycin. Cells were thawed at 37 °C for 1−2 min and placed in 75-flask with 12 mL of fresh media and incubated at 37 °C with 5% CO_2 and 95% humidity for 24−48 h until it reached 80−90% confluence. Further, confluent cells were washed with 5 mL of PBS and incubated with 5 mL of trypsin for 5 min at 37 °C. After that, 10 mL of fresh media was added to stop the trypsin function. Cells were centrifuged at 200×*g* for 5 min. Then, the supernatant was discarded, and the cells were suspended in 5 mL of fresh media. For the cytotoxicity assay, 96-well plates were used, and cells were seeded at 8000 cells/well in 100 μL of media (3 wells were left blank to be used as background control) and incubated overnight at 37 °C with 5% CO_2 and 95% humidity. Then, the cells were treated with different concentrations of the BCM, CHL-BCM, and free drug, making the total volume in each well 200 μL, and incubated for 24 h at 37 °C. Cells without treatment were used as the negative control. After 24 h, the media was discarded by flipping the plate on a clean tissue, and following the manufacturer's protocol for the cell cytotoxicity kit (CCK) test; 10 μL of the CCK reagent was added to 100 μL of fresh media in each well. The cells were incubated for 3−5 h at 37 °C. A microplate reader, Thermo Scientific Varioskan LUX multimode microplate reader, was used to measure the absorbance ratio at two wavelengths of 570 and 605 nm. The average absorbance of blank wells was subtracted from all wells to remove the background noise. Then, the average absorbance of the control (cells with no treatment) was calculated and considered 100% viable, and the viability of other treated cells was calculated using the following formula: Cell viability % = (corrected average absorbance of treated cells)/(corrected average absorbance of control) × 100.

Cellular Uptake and Imaging. Following the previously published protocol,[21] HeLa cells were seeded (6×10^3 cells/well) into a 4-well chamber cover glass and maintained using complete DMEM media overnight in a 5% CO_2 incubator at 37 °C. 100 μg mL^{-1} of BCM was incubated with the cells for live cell imaging from 5 to 60 min. Also, 50 μg mL^{-1} of the BCM and CHL-BCM were incubated with the cells for 4 h at 37 °C. After that, the media was discarded, and cells were washed with PBS three times for 5 min each and fixed by incubating the cells with 4% paraformaldehyde for 30 min at room temperature. The treated cells were observed and imaged using a confocal laser scanning microscope (Leica Stellaris/SP8) following a standard protocol. The uptakes of the BCM and CHL-BCM were detected using three laser channels; excitation/emission (ex/em); [TPE 405/460, RhB 546/590, and energy transfer channel (ETC) 405/590]. Non-treated cells were used as a control to set the intensity and gain as no signal could be detected in the control sample. ImageJ software was used to calculate the corrected total cell fluorescence (CTCF) following the reported formula CTCF = integrated

https://doi.org/10.1021/acsomega.3c01514
ACS Omega 2023, 8, 22698−22707

Scheme 1. Conjugation of RhB to the Block Copolymer *via* Post-Polymerization Modification

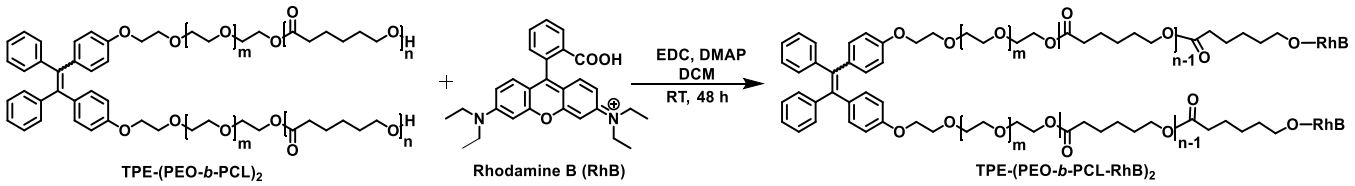

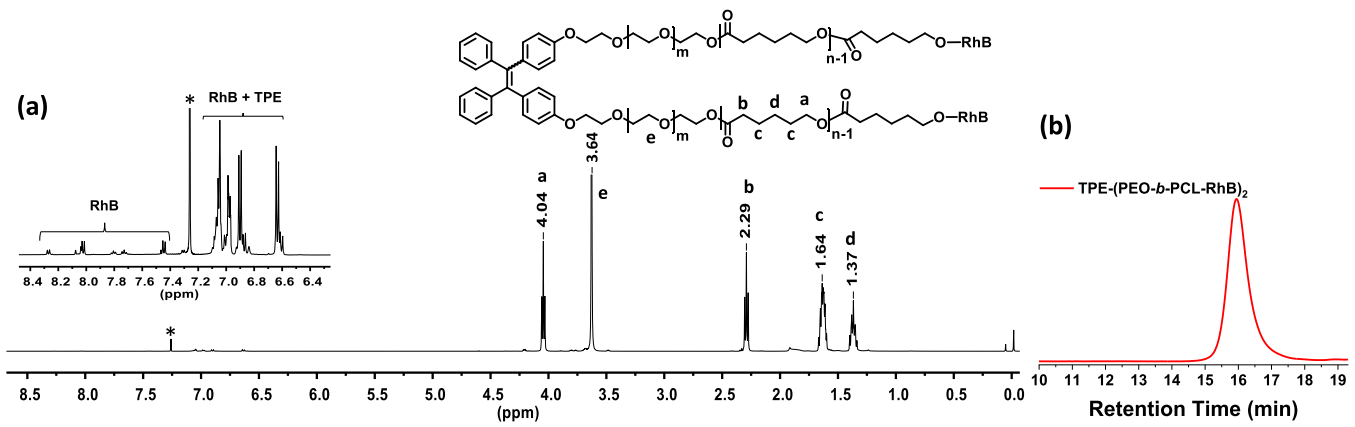

Figure 2. (a) ^{1}H NMR spectrum (500 MHz, $CDCl_3$, 25 °C). (b) SEC chromatogram of TPE-(PEO-*b*-PCL-RhB)$_2$ (DMF, 45 °C, PS standard calibration).

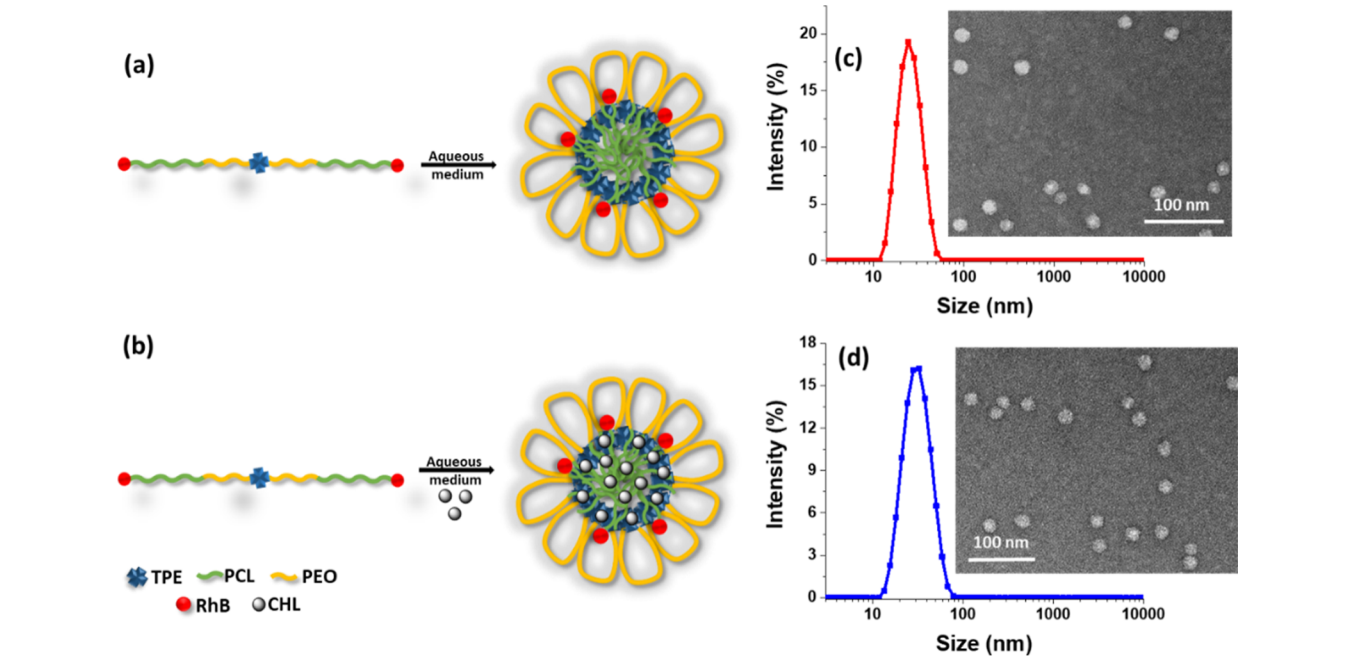

Figure 3. Schematic illustration of self-assembly of (a) BCM and (b) CHL-BCM. DLS measurements (aqueous medium) and TEM images of (c) BCM and (d) CHL-BCM.

density − (area of selected cell × mean fluorescence of background readings).[30]

Flow Cytometry Measurements. To test the efficiency of the uptake, flow cytometry analysis was performed following a previously reported protocol.[31] Briefly, cells were seeded into six-well plates at 4 × 10^5 cells/well and cultured for 12 h in 2 mL of DMEM containing 10% FBS and 1% penicillin−streptomycin. After that, 100 μg mL^{-1} of BCM was incubated with the cells for 1 h; the cells were washed with PBS, detached by trypsin, and collected by centrifugation at 1000 rpm for 5 min. The cells were suspended in complete media and tested by BD LSR Fortessa, and the data were analyzed by Flowjo software.

RESULTS AND DISCUSSION

Post-Polymerization Modification and Self-Assembly. The synthesis and structural characterization of the TPE-(PEO-*b*-PCL)$_2$ block copolymer is described in our previous work.[22] Furthermore, as outlined in Scheme 1, the post-polymerization modification was achieved by facile one-step

https://doi.org/10.1021/acsomega.3c01514
ACS Omega 2023, 8, 22698−22707

Table 1. Hydrodynamic Size and Size Distribution, Drug-Loading Content, and Efficiency of the TPE-(PEO-*b*-PCL-RhB)$_2$ BCM[a]

triblock copolymer	size[b] (nm)	PDI[b]	DLC[c] (%)	DLE (%)
BCM	26.1 ± 0.2	0.066 ± 0.009		
CHL-BCM	32.5 ± 3.0	0.111 ± 0.025	12.6 ± 1.2	50.4 ± 4.8

[a]The results are expressed as mean ± standard deviation (n = 3). [b]Particle size and PDI determined by DLS. [c]Measured by UV−visible spectroscopy.

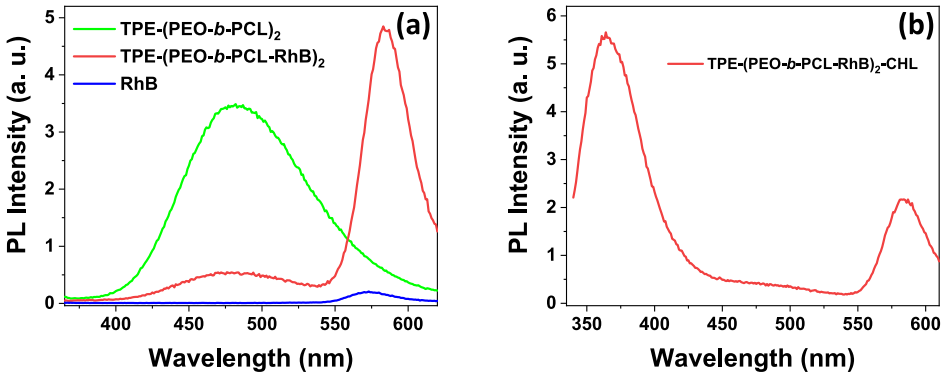

Figure 4. Fluorescence emission spectra (λ_{ex} 315 nm) of (a) BCM [along with TPE-(PEO-*b*-PCL)$_2$ micelles and free RhB] and (b) CHL-BCM in aqueous medium at a concentration of 0.1 mg mL^{-1}.

esterification under mild reaction conditions with a simple purification step. The polymer was further subjected to water dialysis purification to remove unreacted RhB to avoid interfering in the analysis of the covalently attached RhB at the chain-end. NMR and SEC analyses proved the successful synthesis of TPE-(PEO-*b*-PCL-RhB)$_2$. As shown in the ^{1}H NMR spectrum in Figure 2a, the aromatic proton signals from 6.90 to 8.30 ppm belong to the characteristic protons of RhB along with the TPE molecule. The conjugation of RhB with the polymer was achieved with 25% conversion efficiency, calculated by comparing the integrals of the proton signal at 6.60 ppm (from TPE) with the proton signal at 8.27 ppm from RhB. This RhB content is high enough to obtain strong fluorescence for *in vitro* cellular imaging and low enough to avoid cytotoxicity. The SEC chromatogram (Figure 2b) revealed a monomodal peak with narrow molecular weight distribution ($Đ$ = 1.18) confirming the well-defined structure of the polymer.

The inherent amphiphilic framework of the block copolymer favored self-assembly into micelles in an aqueous solution. The BCM were prepared by the co-solvent evaporation method. The critical micelle concentration (CMC) value of TPE-(PEO-*b*-PCL)$_2$ before and after RhB conjugation was determined by fluorescence spectroscopy using pyrene as a hydrophobic probe[32,33] (Figure S3, Supporting Information). The CMC was measured to be 8.0 and 10.0 μg mL^{-1} for TPE-(PEO-*b*-PCL)$_2$ and TPE-(PEO-*b*-PCL-RhB)$_2$, respectively. These results reveal that the CMCs of TPE-(PEO-*b*-PCL)$_2$ before and after RhB conjugation were comparable, suggesting that the self-assembly behavior of TPE-(PEO-*b*-PCL)$_2$ is not affected by the RhB conjugation. As schematically shown in Figure 3, flower-like micelles[22] were formed; the hydrodynamic size and size distribution of the micelles were measured by DLS. As shown in Figure 3c, BCM exhibited an average hydrodynamic diameter of 26.1 ± 0.2 with unimodal size distributions, and TEM analysis revealed the formation of homogeneous spherical micelles. Further, CHL-BCM were prepared following a similar procedure to that for the BCM. The DLC and DLE investigated by UV−Vis spectroscopy were determined to be 12.6 ± 1.2% and 50.4 ± 4.8%, respectively. The CHL-BCM showed (Figure 3d) an average hydrodynamic size of 32.5 ± 3.0 with a narrow size distribution, and a spherical morphology was confirmed by TEM analysis. The details of DLS measurements and drug-loading properties are summarized in Table 1. Thus, the drug-loaded micelles possess enhanced aqueous solubility and bioavailability of CHL. Moreover, the diameter of the micelle is in the desired size range (10−100 nm) to achieve effective accumulation in solid tumors *via* the EPR effect.

Photophysical Study. The photophysical properties of the BCM were investigated as the block copolymer contains two dyes, TPE and RhB. As shown in Figure S4 (Supporting Information), the UV−Vis spectrum of the BCM displayed an absorption peak at 315 nm corresponding to TPE molecules, and RhB exhibited absorption at 560 nm. Furthermore, the spectral overlap between the aggregate emission of TPE (donor) and absorption of RhB (acceptor) satisfies the requirement of the FRET phenomenon[34] (Figure S5, Supporting Information). As shown in Figure 4a, the emission spectrum of BCM, excited at 315 nm (maximum absorbance of TPE), revealed a reduced emission intensity at 475 nm (aggregate emission peak of TPE), whereas RhB exhibited significant emission at 580 nm. Meanwhile, RhB (free dye) molecules showed negligible emission at 580 nm when excited at 315 nm[35] (corresponding to maximum absorbance of TPE). These results suggest that FRET occurred between TPE (donor) and RhB (acceptor). Surprisingly, CHL-BCM revealed a different fluorescence behavior as seen in Figure 4b. The TPE monomer emission peak is observed at 365 nm (λ_{ex} 315 nm), which prevented the fluorescence energy transfer between TPE and RhB. Since there is no significant overlap between the monomeric emission of TPE, and the absorption of the acceptor (RhB) for the energy transfer process to take place. The monomeric emission of TPE could be attributed to the confinement of the CHL molecule between two TPE molecules, preventing aggregate formation, and the rotation of

https://doi.org/10.1021/acsomega.3c01514
ACS Omega 2023, 8, 22698−22707

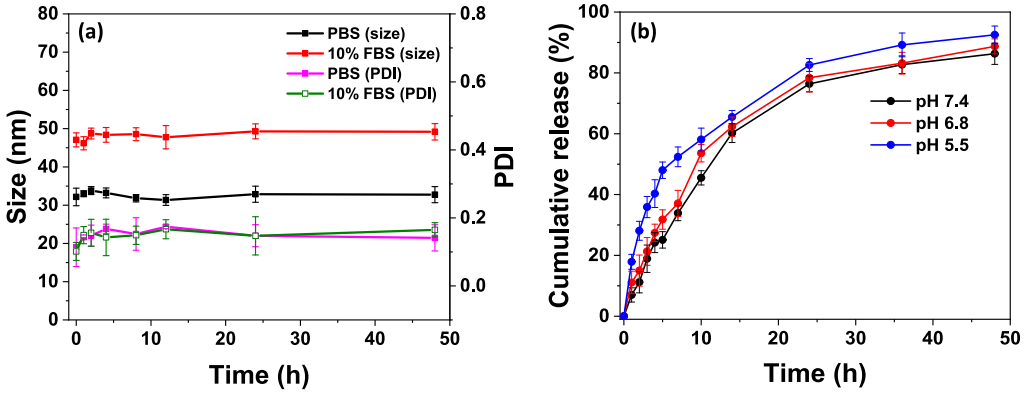

Figure 5. (a) Stability of CHL-BCM in PBS (pH 7.4) and PBS (pH 7.4) containing 10% FBS incubated at 37 °C. (b) *In vitro* CHL release from BCM at pH 7.4, 6.8, and 5.5 (37 °C). The results are presented as average ± standard deviation (n = 3).

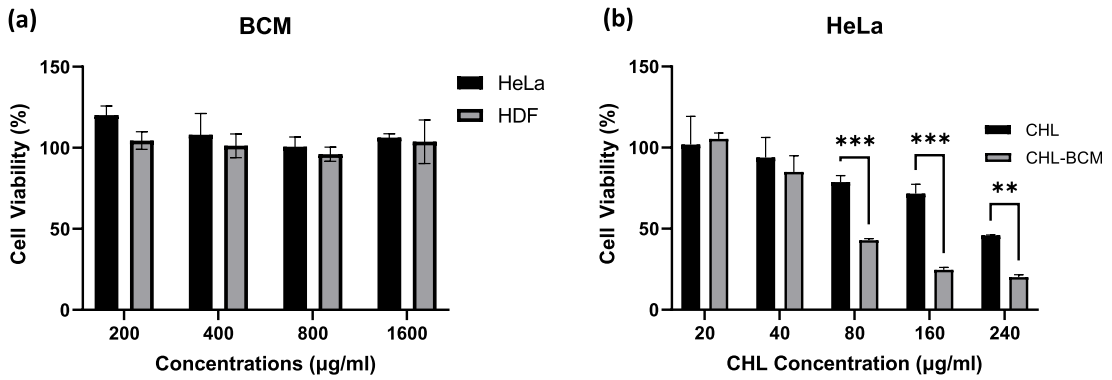

Figure 6. Viability after 24 h of incubation of (a) HeLa and HDF cells with different concentrations of BCM and (b) HeLa cells with different concentrations of the free drug (CHL) and CHL-BCM. Error bars are based on SD (n = 3). Statistical significance was calculated by two-way ANOVA *P < 0.01, **P < 0.001, ***P < 0.0001.

phenyl rings is restricted as TPE is present at the hydrophobic core of the micelles. In order to prove this, fluorescence spectra were determined (λ_{ex} 315 nm) at different loading amounts of CHL into the micelles, as shown in Figure S6 (Supporting Information). With the increasing amount of CHL, the monomeric emission of TPE increases along with the decrease of RhB emission. The enhancement of monomeric emission in the case of the increasing amount of CHL clearly indicates that it resulted from the confinement of CHL between TPE molecules, which eventually reduced the FRET effect between TPE and RhB. The block copolymer in the present study was designed to develop a FRET probe to study the real-time monitoring of CHL delivery at the cellular level. However, based on the above results, eventually, RhB was utilized as a fluorescent probe for visualizing the *in vitro* cellular uptake of CHL-BCM though the loading of CHL diminished the FRET effect.

Stability and *In Vitro* Drug Release Study. The stability of CHL-BCM was investigated by DLS in PBS (pH 7.4) and 10% FBS for 48 h. As shown in Figure 5a, the micelles did not show any significant change in the hydrodynamic diameter and PDI. A particle size of 30−34 nm in PBS and 45−50 nm in 10% FBS with low PDI values was constantly maintained over 48 h, suggesting that CHL-BCM possess good stability. Subsequently, the *in vitro* drug release from the polymer micelles was investigated at the physiological pH of 7.4 as well as at the acidic pH of 6.8 and 5.5 corresponding to the pH of the tumor microenvironment and intracellular acidic pH by the dialysis method. The drug release profiles are shown in Figure 5b. Under all conditions, a relatively rapid release of CHL up to 14 h followed by sustained drug release (from 14 to 48 h) was observed. The sustained release of CHL could probably be attributed to the $\pi-\pi$ stacking between the CHL and TPE molecules and provides an opportunity to maintain its effective concentration in the body and continually inhibit the proliferation of the cancer cells. Further, in the first 14 h, 60.2, 62.3, and 65.5% of drug was released at pH 7.4, 6.8, and 5.5, respectively. Also, at the end of 48 h, drug releases of 86.3, 88.7, and 92.5% were obtained for pH 7.4, 6.8, and 5.5, respectively. A relatively faster release of CHL was observed in acidic conditions (drug release at pH 7.4 < 6.8 < 5.5), which could be attributed to the higher solubility of CHL in the acidic condition than that of the neutral condition.[36] In order to investigate the mechanism of CHL release from the micelles, the release data (up to 60% of the total release) were fitted with the Korsmeyer−Peppas model as shown in equation[37]

$$\frac{M_t}{M_\infty} = kt^n$$

Here, M_t and M_∞ are the cumulative drug release at time t and infinite time, respectively, k is a release rate constant, and n is the release exponent indicative of the drug release mechanism. For spherical particles, n = 0.43, indicating Fickian diffusion or case-I diffusion and n = 0.85, indicating case-II diffusion. For the case 0.43 < n < 0.85, non-Fickian (anomalous) diffusion is observed.[38] The corresponding graph of the Korsmeyer−Peppas equation for the drug release data revealed a good

https://doi.org/10.1021/acsomega.3c01514
ACS Omega 2023, 8, 22698−22707

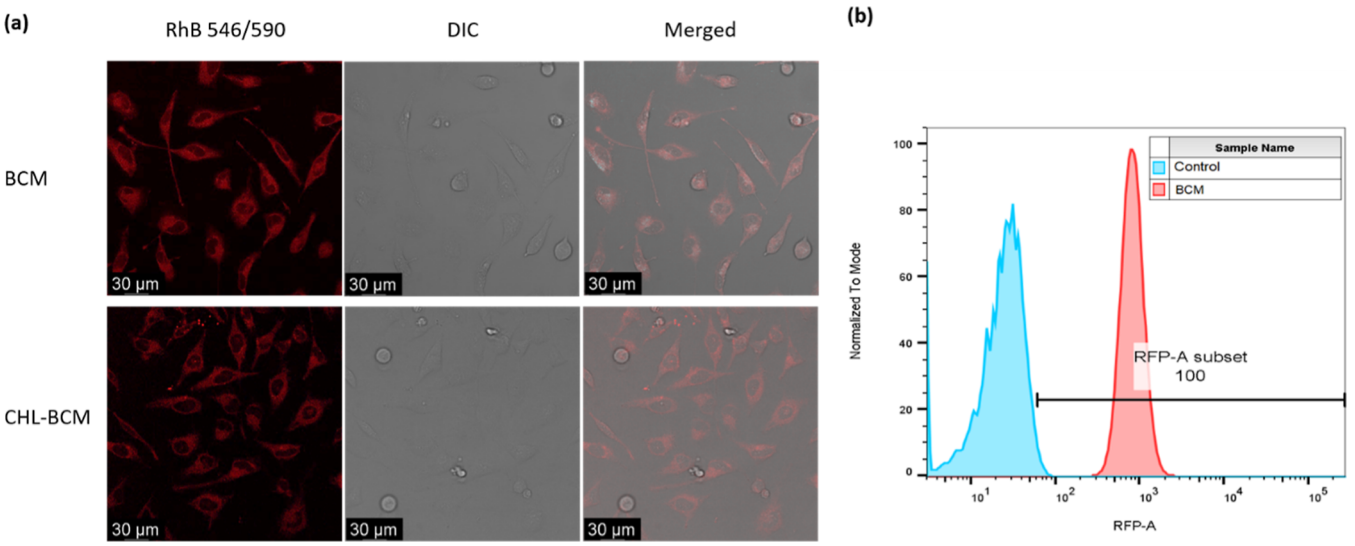

Figure 7. (a) CLSM images of the uptake of 50 μg mL^{-1} of BCM and CHL-BCM excited at 546 nm and received at 590 ± 10 nm with HeLa cells after 4 h of incubation. (b) Representative flow cytometry plots of HeLa cells treated with BCM for 1 h in comparison to untreated cells (control) using the RFP channel (546/590).

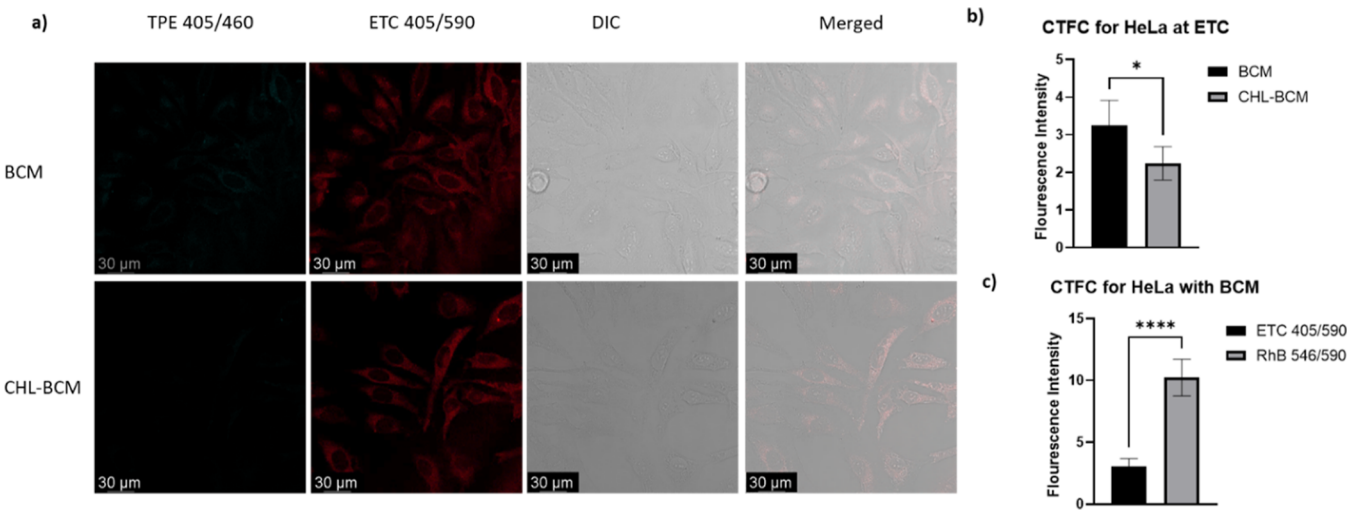

Figure 8. (a) CLSM images of the uptake of 50 μg mL^{-1} of BCM and CHL-BCM with HeLa cells after 4 h of incubation, excited at the TPE channel (405/460) and ETC (405/590). Comparison of the (b) CTCF intensity of the RhB fluorescence signal using the ETC in HeLa cells when incubated with BCM and CHL-BCM for 4 h and (c) CTCF intensity of BCM in HeLa cells using ETC (405/590) and the RhB (546/590) laser channel. Error bars are based on SD (n = 6). Statistical significance was calculated by an unpaired t-test *P < 0.01, **P < 0.001, ***P < 0.0001.

linear fitting (shown in Figure S7, Supporting Information). The release kinetics parameters as summarized in Table S1 (Supporting Information) showed release exponent values n = 0.82, 0.68, and 0.51 for pH 7.4, 6.8, and 5.5, respectively. These results suggest that the release of CHL from the micelles followed a non-Fickian diffusion or anomalous transport mechanism. Thus, drug release was controlled by a combined effect of diffusion and the disaggregation of a fraction of micelles due to the presence of acetonitrile (5% v/v), which is used as the co-solvent to improve the solubility of the released CHL in PBS. Therefore, in the present case, both the factors micelle disaggregation and drug diffusion are involved in the drug release mechanism.[39]

Cytotoxicity Study. After proving the release behavior of CHL-BCM, it was essential to study its toxicity with different cell lines to be used for biomedical applications. The BCM was incubated with cancerous (HeLa) and normal (HDF) cell lines using different concentrations (200−1600 μg mL^{-1}) for 24 h. The CCK was used to quantify cells' growth and inhibition. As shown in Figure 6a, BCM showed very high biocompatibility[40,41] toward HeLa and HDF cells up to 1600 μg mL^{-1} and promoted their growth as well. These results prove that the block copolymer is nontoxic and can promote cellular growth, which makes them suitable for biomedical applications. Subsequently, the CHL drug was used as a model for anticancer drug to be loaded into the block copolymer. CHL is a lipophilic drug that is used against many types of cancers as it can damage the DNA and inhibit cells' proliferation.[42] It has low water solubility and low stability in biological medium; therefore, loading CHL into the block copolymer enhanced its solubility and protected it from degradation, which would enhance the efficacy of the drug.[43] Different concentrations of free and loaded CHL (ranging from 20 to 240 μg mL^{-1}) were incubated with HeLa and HDF cells for 24 h. As presented in

https://doi.org/10.1021/acsomega.3c01514
ACS Omega 2023, 8, 22698−22707

Figures 6b and S8 (Supporting Information), the loaded CHL caused a significant inhibition in the proliferation of HeLa and HDF cells in comparison to free CHL. The loading had enhanced the potency of the drug by more than three-fold as the IC_{50} of the loaded drug was 80 μg mL^{-1}, whereas for the free CHL, it was more than 240 μg mL^{-1}. This proves the successful delivery and protection of CHL, which leads to enhanced efficacy as expected.

Cellular Uptake and Imaging Study. The cellular internalization is an important criterion for polymer micelles to realize their anticancer activity. Therefore, we investigated the cellular uptake of the BCM and CHL-BCM and their localization inside the cells using CLSM. The presence of RhB eased the tracking and imaging of the polymer micelles inside the cells. Live cell images were taken after 5, 30, and 60 min of incubation of BCM with HeLa cells for up to 60 min. As shown in Figure S9 (Supporting Information), a bright red fluorescence can be clearly seen inside the cells after 5 min of incubation with an increase in intensity over time. These observations indicate the rapid internalization of BCM, which is required in anticancer treatment to minimize the side effects of the used drugs. Moreover, as shown in Figure 7a, the high red fluorescence signal of RhB can be easily seen in the cytoplasm and perinuclear area after 4 h of incubating BCM with HeLa cells when excited at the RhB channel Ex/Em (546/590 nm). Similar fluorescence and localization patterns were observed for the drug-loaded micelles CHL-BCM in comparison to BCM, as shown in Figure 7a. Furthermore, flow cytometry analysis was performed to quantify the efficiency of BCM cellular uptake. As shown in Figure 7b, BCM showed very high efficiency as all treated cells exhibited red fluorescence when excited at 546 nm using the red fluorescent protein (RFP) channel.

In line with the fluorescence spectra and energy transfer theory, using the laser at the ETC (405/590) where the excitation occurs at the donor channel and emission is collected at the accepter channel, both BCM and CHL-BCM gave the red fluorescence signal of RhB as presented in Figure 8a. However, the CTCF of BCM was higher than that of CHL-BCM as CHL affected the energy transfer, as explained earlier (Figure 8b). Moreover, the RhB signal was more than three-fold higher using the RhB channel than the fluorescence intensity using the ETC (Figure 8c). Therefore, the RhB channel is a better choice when imaging the internalization of the polymer due to its excellent fluorescent property. Overall, TPE-(PEO-*b*-PCL-RhB)$_2$ is a promising candidate for imaging and drug delivery as it showed superior biocompatibility, fast cellular uptake, and excellent fluorescence properties.

CONCLUSIONS

In this paper, we present a facile method to fabricate BCM with RhB fluorescent probe and CHL anticancer drug for imaging and potential anticancer drug delivery to cancer cells. The fluorescent probe RhB-conjugated triblock copolymer TPE-(PEO-*b*-PCL-RhB)$_2$ was synthesized from the triblock by a simple post-polymerization modification. The block copolymer is easily self-assembled into micelles in an aqueous medium thanks to its amphiphilicity. Furthermore, CHL was successfully loaded (with a loading capacity of 12.6 ± 1.2%) into the block copolymer micelles to enhance its aqueous solubility. The BCM and CHL-BCM, characterized by DLS and TEM, exhibited a favorable size for the passive targeting of tumor tissues through the EPR effect. The photophysical properties of the BCM and CHL-BCM were studied. The emission spectrum (λ_{ex} 315 nm) of BCM demonstrates energy transfer from aggregated TPE molecules to RhB. In contrast, CHL-BCM exhibits monomeric emission of TPE (λ_{ex} 315 nm) due to the $\pi-\pi$ stacking between TPE and CHL molecules. The *in vitro* drug release profile displayed sustained drug release for 48 h. The biocompatibility of BCM and cytotoxicity of CHL-BCM toward cancer cells ensured the capability of the block copolymer as a drug nanocarrier. Furthermore, the cellular uptake by CLSM studies utilizing RhB fluorescent probe illustrates that BCM and CHL-BCM effectively internalize into the cancer cells. Therefore, these results indicate that the BCM holds great potential for theranostic applications.

ASSOCIATED CONTENT

Supporting Information

The Supporting Information is available free of charge at https://pubs.acs.org/doi/10.1021/acsomega.3c01514.

CHL calibration plot, NMR spectrum, CMC plots, UV–Vis and fluorescence emission spectra, drug release kinetics, cell viability plot, and CLSM images (PDF)

AUTHOR INFORMATION

Corresponding Authors

Niveen M. Khashab − *Smart Hybrid Materials (SHMs) Laboratory, Chemistry Program, Advanced Membranes and Porous Materials Center, King Abdullah University of Science and Technology (KAUST), Thuwal 23955-6900, Saudi Arabia;* orcid.org/0000-0003-2728-0666; Email: niveen.khashab@kaust.edu.sa

Nikos Hadjichristidis − *Polymer Synthesis Laboratory, Chemistry Program, KAUST Catalysis Center, Physical Sciences and Engineering Division, King Abdullah University of Science and Technology (KAUST), Thuwal 23955, Saudi Arabia;* orcid.org/0000-0003-1442-1714; Email: nikolaos.hadjichristidis@kaust.edu.sa

Authors

Bhagyashree Kulkarni − *Polymer Synthesis Laboratory, Chemistry Program, KAUST Catalysis Center, Physical Sciences and Engineering Division, King Abdullah University of Science and Technology (KAUST), Thuwal 23955, Saudi Arabia*

Somayah Qutub − *Smart Hybrid Materials (SHMs) Laboratory, Chemistry Program, Advanced Membranes and Porous Materials Center, King Abdullah University of Science and Technology (KAUST), Thuwal 23955-6900, Saudi Arabia*

Complete contact information is available at: https://pubs.acs.org/10.1021/acsomega.3c01514

Notes

The authors declare no competing financial interest.

ACKNOWLEDGMENTS

The research reported in this publication was supported by the King Abdullah University of Science and Technology (KAUST).

REFERENCES

(1) Robak, T.; Kasznicki, M. Alkylating agents and nucleoside analogues in the treatment of B cell chronic lymphocytic leukemia. *Leukemia* **2002**, *16*, 1015−1027.

(2) Millard, M.; Gallagher, J. D.; Olenyuk, B. Z.; Neamati, N. A Selective Mitochondrial-Targeted Chlorambucil with Remarkable Cytotoxicity in Breast and Pancreatic Cancers. *J. Med. Chem.* **2013**, *56*, 9170−9179.

(3) Horton, J. K.; Roy, G.; Piper, J. T.; Van Houten, B.; Awasthi, Y. C.; Mitra, S.; Alaoui-Jamali, M. A.; Boldogh, I.; Singhal, S. S. Characterization of a chlorambucil-resistant human ovarian carcinoma cell line overexpressing glutathione S-transferase μ. *Biochem. Pharmacol.* **1999**, *58*, 693−702.

(4) Mattes, W. B.; Hartley, J. A.; Kohn, K. W. DNA sequence selectivity of guanine-N7 alkylation by nitrogen mustards. *Nucleic Acids Res.* **1986**, *14*, 2971−2987.

(5) Polavarapu, A.; Stillabower, J. A.; Stubblefield, S. G. W.; Taylor, W. M.; Baik, M.-H. The Mechanism of Guanine Alkylation by Nitrogen Mustards: A Computational Study. *J. Org. Chem.* **2012**, *77*, 5914−5921.

(6) Tadros, M. I.; Al-mahallawi, A. M. Long-circulating lipoprotein-mimic nanoparticles for smart intravenous delivery of a practically-insoluble antineoplastic drug: Development, preliminary safety evaluations and preclinical pharmacokinetic studies. *Int. J. Pharm.* **2015**, *493*, 439−450.

(7) Reux, B.; Weber, V.; Galmier, M.-J.; Borel, M.; Madesclaire, M.; Madelmont, J.-C.; Debiton, E.; Coudert, P. Synthesis and cytotoxic properties of new fluorodeoxyglucose-coupled chlorambucil derivatives. *Bioorg. Med. Chem.* **2008**, *16*, 5004−5020.

(8) Sanderson, B. J. S.; Shield, A. J. Mutagenic damage to mammalian cells by therapeutic alkylating agents. *Mutat. Res., Fundam. Mol. Mech. Mutagen.* **1996**, *355*, 41−57.

(9) Cabral, H.; Miyata, K.; Osada, K.; Kataoka, K. Block Copolymer Micelles in Nanomedicine Applications. *Chem. Rev.* **2018**, *118*, 6844−6892.

(10) Biswas, G.; Jena, B. C.; Maiti, S.; Samanta, P.; Mandal, M.; Dhara, D. Photoresponsive Block Copolymer Prodrug Nanoparticles as Delivery Vehicle for Single and Dual Anticancer Drugs. *ACS Omega* **2017**, *2*, 6677−6690.

(11) Saha, B.; Bhattacharyya, S.; Mete, S.; Mukherjee, A.; De, P. Redox-Driven Disassembly of Polymer−Chlorambucil Polyprodrug: Delivery of Anticancer Nitrogen Mustard and DNA Alkylation. *ACS Appl. Polym. Mater.* **2019**, *1*, 2503−2515.

(12) Cabral, H.; Kataoka, K. Progress of drug-loaded polymeric micelles into clinical studies. *J. Contr. Release* **2014**, *190*, 465−476.

(13) Pradeepkumar, P.; Rajendran, N. K.; Alarfaj, A. A.; Munusamy, M. A.; Rajan, M. Deep Eutectic Solvent-Mediated FA-g-β-Alanine-co-PCL Drug Carrier for Sustainable and Site-Specific Drug Delivery. *ACS Appl. Bio Mater.* **2018**, *1*, 2094−2109.

(14) Mukherjee, S.; Das Sarma, J.; Shunmugam, R. pH-Sensitive Nanoaggregates for Site-Specific Drug-Delivery as Well as Cancer Cell Imaging. *ACS Omega* **2016**, *1*, 755−764.

(15) Gangopadhyay, M.; Singh, T.; Behara, K. K.; Karwa, S.; Ghosh, S. K.; Singh, N. D. P. Coumarin-containing-star-shaped 4-arm-polyethylene glycol: targeted fluorescent organic nanoparticles for dual treatment of photodynamic therapy and chemotherapy. *Photochem. Photobiol. Sci.* **2015**, *14*, 1329−1336.

(16) Karthik, S.; Jana, A.; Selvakumar, M.; Venkatesh, Y.; Paul, A.; Shah, S. S.; Singh, N. D. P. Coumarin polycaprolactone polymeric nanoparticles: light and tumor microenvironment activated cocktail drug delivery. *J. Mater. Chem. B* **2017**, *5*, 1734−1741.

(17) Liu, B.-Y.; Wu, W.-X.; Liu, Y.-H.; Jia, C.; Yang, X.-L.; Li, J.; Wang, N.; Yu, X.-Q. Water-soluble mitochondria-targeting polymeric prodrug micelles for fluorescence monitoring and high intracellular anticancer efficiency. *Polym. Chem.* **2017**, *8*, 5982−5987.

(18) Liu, B.-Y.; Yang, X.-L.; Xing, X.; Li, J.; Liu, Y.-H.; Wang, N.; Yu, X.-Q. Trackable Water-Soluble Prodrug Micelles Capable of Rapid Mitochondrial-Targeting and Alkaline pH-Responsive Drug Release for Highly Improved Anticancer Efficacy. *ACS Macro Lett.* **2019**, *8*, 719−723.

(19) Patra, D.; Kumar, P.; Samanta, T.; Chakraborty, I.; Shunmugam, R. Coordinately Tethered Iron(III) Fluorescent Nanotheranostic Polymer Ascertaining Cancer Cell Mitochondria Destined Potential Chemotherapy and T1-Weighted MRI Competency. *ACS Appl. Bio Mater.* **2022**, *5*, 1284−1296.

(20) Pang, Y.; Zhu, Q.; Liu, J.; Wu, J.; Wang, R.; Chen, S.; Zhu, X.; Yan, D.; Huang, W.; Zhu, B. Design and Synthesis of Cationic Drug Carriers Based on Hyperbranched Poly(amine-ester)s. *Biomacromolecules* **2010**, *11*, 575−582.

(21) Saha, B.; Haldar, U.; De, P. Polymer-Chlorambucil Drug Conjugates: A Dynamic Platform of Anticancer Drug Delivery. *Macromol. Rapid Commun.* **2016**, *37*, 1015−1020.

(22) Kulkarni, B.; Qutub, S.; Ladelta, V.; Khashab, N. M.; Hadjichristidis, N. AIE-Based Fluorescent Triblock Copolymer Micelles for Simultaneous Drug Delivery and Intracellular Imaging. *Biomacromolecules* **2021**, *22*, 5243−5255.

(23) Yang, L.; Cui, C.; Wang, L.; Lei, J.; Zhang, J. Dual-Shell Fluorescent Nanoparticles for Self-Monitoring of pH-Responsive Molecule-Releasing in a Visualized Way. *ACS Appl. Mater. Interfaces* **2016**, *8*, 19084−19091.

(24) Xue, Y.; Lee, J.; Kim, H.-J.; Cho, H.-J.; Zhou, X.; Liu, Y.; Tebon, P.; Hoffman, T.; Qu, M.; Ling, H.; Jiang, X.; Li, Z.; Zhang, S.; Sun, W.; Ahadian, S.; Dokmeci, M. R.; Lee, K.; Khademhosseini, A. Rhodamine Conjugated Gelatin Methacryloyl Nanoparticles for Stable Cell Imaging. *ACS Appl. Bio Mater.* **2020**, *3*, 6908−6918.

(25) Maeda, H.; Wu, J.; Sawa, T.; Matsumura, Y.; Hori, K. Tumor vascular permeability and the EPR effect in macromolecular therapeutics: a review. *J. Contr. Release* **2000**, *65*, 271−284.

(26) Aliabadi, H. M.; Elhasi, S.; Mahmud, A.; Gulamhusein, R.; Mahdipoor, P.; Lavasanifar, A. Encapsulation of hydrophobic drugs in polymeric micelles through co-solvent evaporation: The effect of solvent composition on micellar properties and drug loading. *Int. J. Pharm.* **2007**, *329*, 158−165.

(27) Kulkarni, B.; Surnar, B.; Jayakannan, M. Dual Functional Nanocarrier for Cellular Imaging and Drug Delivery in Cancer Cells Based on pi-Conjugated Core and Biodegradable Polymer Arms. *Biomacromolecules* **2016**, *17*, 1004−1016.

(28) Zhu, W.; Song, Z.; Wei, P.; Meng, N.; Teng, F.; Yang, F.; Liu, N.; Feng, R. Y-shaped biotin-conjugated poly (ethylene glycol)−poly (epsilon-caprolactone) copolymer for the targeted delivery of curcumin. *J. Colloid Interface Sci.* **2015**, *443*, 1−7.

(29) Alexis, F.; Venkatraman, S. S.; Rath, S. K.; Boey, F. In vitro study of release mechanisms of paclitaxel and rapamycin from drug-incorporated biodegradable stent matrices. *J. Contr. Release* **2004**, *98*, 67−74.

(30) GitHub. Measuring Cell Fluorescence Using ImageJ. https://theolb.readthedocs.io/en/latest/imaging/measuring-cell-fluorescence-using-imagej.html.

(31) Alsaiari, S. K.; Qutub, S. S.; Sun, S.; Baslyman, W.; Aldehaiman, M.; Alyami, M.; Almalik, A.; Halwani, R.; Merzaban, J.; Mao, Z.; Khashab, N. M. Sustained and targeted delivery of checkpoint inhibitors by metal-organic frameworks for cancer immunotherapy. *Sci. Adv.* **2021**, *7*, No. eabe7174.

(32) Jia, M.; Zhang, D.; Gnanou, Y.; Feng, X. Surfactant-Emulating Amphiphilic Polycarbonates and Other Functional Polycarbonates through Metal-Free Copolymerization of CO2 with Ethylene Oxide. *ACS Sustain. Chem. Eng.* **2021**, *9*, 10370−10380.

(33) Xia, Y.; Yao, H.; Miao, Z.; Ma, Y.; Cui, M.; Yan, L.; Ling, H.; Qi, Z. Facile synthesis and self-assembly of amphiphilic polydimethylsiloxane with poly(ethylene glycol) moieties via thiol-ene click reaction. *RSC Adv.* **2015**, *5*, 50955−50961.

(34) Kulkarni, B.; Jayakannan, M. Fluorescent-Tagged Biodegradable Polycaprolactone Block Copolymer FRET Probe for Intracellular Bioimaging in Cancer Cells. *ACS Biomater. Sci. Eng.* **2017**, *3*, 2185−2197.

(35) Xue, X.; Jin, S.; Li, Z.; Zhang, C.; Guo, W.; Hu, L.; Wang, P. C.; Zhang, J.; Liang, X.-J. Through-Bond Energy Transfer Cassette with

https://doi.org/10.1021/acsomega.3c01514
ACS Omega 2023, 8, 22698−22707

Dual-Stokes Shifts for "Double Checked" Cell Imaging. *Adv. Sci.* **2017**, *4*, 1700229.
(36) Singh, G.; Nenavathu, B. P.; Imtiyaz, K.; Moshahid A Rizvi, M. Fabrication of chlorambucil loaded graphene- oxide nanocarrier and its application for improved antitumor activity. *Biomed. Pharmacother.* **2020**, *129*, 110443.
(37) Gao, Y.; Chang, M.-W.; Ahmad, Z.; Li, J.-S. Magnetic-responsive microparticles with customized porosity for drug delivery. *RSC Adv.* **2016**, *6*, 88157−88167.
(38) Siepmann, J.; Peppas, N. A. Modeling of drug release from delivery systems based on hydroxypropyl methylcellulose (HPMC). *Adv. Drug Deliv. Rev.* **2001**, *48*, 139−157.
(39) San Miguel, V.; Limer, A. J.; Haddleton, D. M.; Catalina, F.; Peinado, C. Biodegradable and thermoresponsive micelles of triblock copolymers based on 2-(N,N-dimethylamino)ethyl methacrylate and ε-caprolactone for controlled drug delivery. *Eur. Polym. J.* **2008**, *44*, 3853−3863.
(40) Cai, S.; Vijayan, K.; Cheng, D.; Lima, E. M.; Discher, D. E. Micelles of Different Morphologies—Advantages of Worm-like Filomicelles of PEO-PCL in Paclitaxel Delivery. *Pharm. Res.* **2007**, *24*, 2099−2109.
(41) Ponjavic, M.; Nikolic, M. S.; Nikodinovic-Runic, J.; Ilic-Tomic, T.; Djonlagic, J. Controlled drug release carriers based on PCL/PEO/PCL block copolymers. *Int. J. Polym. Mater. Polym. Biomater.* **2019**, *68*, 308−318.
(42) Yordanov, G. G.; Bedzhova, Z. A.; Dushkin, C. D. Preparation and physicochemical characterization of novel chlorambucil-loaded nanoparticles of poly(butylcyanoacrylate). *Colloid Polym. Sci.* **2010**, *288*, 893−899.
(43) Pineda, F. P.; Ortega-Castro, J.; Alvarez-Idaboy, J. R.; Frau, J.; Cabrera, B. M.; Ramírez, J. C.; Donoso, J.; Muñoz, F. Hydrolysis of a Chlorambucil Analogue. A DFT study. *J. Phys. Chem. A* **2011**, *115*, 2359−2366.

https://doi.org/10.1021/acsomega.3c01514
ACS Omega 2023, 8, 22698−22707